Trans. Japan Soc. Aero. Space Sci.
Vol. 66, No. 6, pp. 187–198, 2023
DOI: 10.2322/tjsass.66.187

Random Generation of Aerodynamic Derivatives for Monte Carlo Evaluation*

Toshikazu MOTODA†

Aviation Technology Directorate, Japan Aerospace Exploration Agency, Mitaka, Tokyo 181–0015, Japan

Monte Carlo simulation (MCS) has been widely applied in the preflight evaluation of flight systems because of advantages such as its ability to evaluate nonlinear systems with uncertain parameters, which are incorporated into MCS randomly and simultaneously. Some aerodynamic and control derivatives can have significant effects on flight control and vehicle performance, so it is important to evaluate the influences of their uncertainties. However, it has not been easy to incorporate uncertainties of derivatives into MCS appropriately. A derivative is the slope of a curve, such as the C_m–α curve. To randomly vary it for use in MCS, the rotation point on the curve must be determined. However, the deviation from the nominal curve becomes greater as the flight condition, such as α, moves further from the rotation point, which can result in excessive variance of the aerodynamic coefficient. This paper presents a new method to generate derivative and bias uncertainties randomly using a covariance matrix of uncertain parameters. The method is applied to the MCS of an existing experimental flight system, and the MCS results are compared with a result that excludes derivative uncertainties to show how to apply the presented method.

Key Words: Monte Carlo Simulation, Uncertainty, Aerodynamic Derivative, Flight Control

Nomenclature

C_D: drag coefficient
C_L: lift coefficient
$C_{L\cdot\alpha}$: stability derivative of C_L with respect to α
C_m: pitching moment coefficient
$C_{m\cdot\alpha}$: stability derivative of C_m with respect to α
$C_{m\cdot\delta e}$: control derivative of C_m with respect to δe
$E[\ ]$: expectation
$\boldsymbol{I}$: identity matrix
J: cost function
M: number of uncertain parameters
N: number of simulations for MCS
$\mathbb{N}$: standard normal distribution
P: conversion matrix for correlated random samples
R: correlation matrix for Σ
S_{mean}: mean value for $\sqrt{V_{cm}}$
V: variance
$V_{g\cdot T}$: touchdown ground speed
X: matrix for state variable data
X_T: touchdown position along runway
Y_T: touchdown position normal to the center of runway
$\dot{Z}_T$: touchdown sink rate
m, n: number of data items
p: number of independent parameters
$\boldsymbol{r}$: vector for correlated normal random sample
$\boldsymbol{u}$: vector for normal random sample
$v_{LD\cdot 0}$: covariance for $\Delta C_{L\cdot 0}$ and $\Delta C_{D\cdot 0}$
$v_{LD\cdot\alpha}$: covariance for $\Delta C_{L\cdot\alpha}$ and $\Delta C_{D\cdot 0}$
$\boldsymbol{x}$: state variable vector
Δ: deviation from nominal value
Θ_T: touchdown pitch angle
Σ: covariance matrix
Φ_T: touchdown roll angle
α: angle of attack
$\boldsymbol{\beta}$: uncertain parameter vector
$\hat{\boldsymbol{\beta}}$: estimation for $\boldsymbol{\beta}$
$\beta_{g\cdot T}$: touchdown sideslip angle with respect to ground speed
δe: elevator angle
δe_{trim}: elevator angle in trimmed flight
$\boldsymbol{\varepsilon}$: residual vector
ρ: correlation coefficient
σ: standard deviation

Subscripts

0: bias for aerodynamic coefficient
A: generalized aerodynamic coefficient
CA: parameter for C_A
D: parameter for C_D
L: parameter for C_L
cm: parameter for C_m
e: parameter for δe
nom: nominal aerodynamic curve
req: requirement
α: parameter for α

1. Introduction

With the rapid increase in computer performance, Monte Carlo simulation (MCS) has come to be widely used in the

*Presented at the 58–60th Aircraft Symposium, 2020–2022, Japan.
Received 31 January 2023; final revision received 5 June 2023; accepted for publication 19 June 2023.

†Corresponding author, motoda.toshikazu@jaxa.jp

development of flight vehicles to confirm system design and for preflight evaluation. In 1996, MCS was applied to the development of an automatic landing system,[1] when it took about 20 h to calculate 1,000 runs of MCS to simulate a real flight time of around 60 s. Despite this, the effectiveness and usefulness of MCS was recognized, and it has increasingly become a useful tool for system evaluation as computer power has increased, including application to successful flight development studies, projects including a lunar landing experiment,[2] and balloon-launched drop tests for transonic and supersonic flight experiments.[3,4] The problem of high computational load can be alleviated by parallel processing,[5] which has become increasingly feasible as the cost of powerful computers has plummeted. Advantages of MCS are its capability to directly evaluate nonlinear systems, and the fact that its results reflect various combinations of input parameters because a number of uncertain parameters are incorporated simultaneously. Because of this, however, it was difficult to find influential uncertain input parameters although MCS outputs are reliable, so methods of detecting influential inputs in MCS have been studied and developed.[6–9] In Motoda and Miyazawa,[6] "Test Input" vectors were created by randomly selecting the elements of uncertain input vectors that caused MCS "failure" results. MCS was then performed using those Test Input vectors, and a statistical test applied to the results to detect the influential parameters. However, Motoda and Miyazawa,[6] applied a statistical test for a hyper-geometric distribution[10] that requires specific software, and an approximated method that does not use that specific software was presented by Motoda.[7] These detection methods require MCS to be performed in the detection process, which takes considerable time. Since practical development requires that the design phase be completed within a given period of time, quick detection methods that skip MCS calculation have been presented. Restrepo and Hurtado[8] applies a pattern recognition algorithm[11] in the early design stages where there tends to be a larger number of failure cases in MCS results. Motoda[9] developed another quick method that is valid for the later design stages where the design has become more refined and there are fewer MCS failures. In this method, input data corresponding to MCS failure results are compared to and statistically tested with a predetermined distribution (population) using both Kuiper's test[12,13] and Z-test.[14] Furthermore, MCS has also been applied to control system design, where design parameters are optimized to minimize the probability of failure.[15–17]

Variation of aerodynamic characteristics has a considerable influence on flight motion, and some aerodynamic and control derivatives such as $C_{m\cdot\alpha}$ and $C_{m\cdot\delta e}$ are well-known to be important and influential parameters for flight control performance. It is therefore important to incorporate uncertainties of the derivatives in addition to bias variations such as $C_{m\cdot 0}$ into MCS for a reliable flight system evaluation. However, incorporating derivative uncertainties into MCS appropriately for flight system evaluation has been problematic. A derivative is the slope of an aerodynamic curve, and needs to be randomly varied. However, when the slope is varied randomly together with a random bias, the variance of the corresponding aerodynamic coefficient, such as C_m, might be excessive. Furthermore, it has been difficult to manage the variance of the coefficient within a realistic range.

Although MCS has become an important and useful tool for flight system development, the appropriate evaluation of derivative uncertainties has remained an unsolved problem. This paper presents a new method to generate random aerodynamic curves for MCS including derivative uncertainties. This is done by introducing correlations of derivatives and bias uncertainties to generate random aerodynamic curves to give a realistic variance of the corresponding aerodynamic coefficient. Finally, the method is applied to the MCS of an existing experimental flight vehicle model in order to show an example of its application.

2. Problem

It has been hard to incorporate aerodynamic derivatives into MCS flight models because of the difficulty of generating their random inputs. MCS is first described in this section, then the problem is discussed.

2.1. Monte Carlo simulation (MCS)

The MCS process is shown in Fig. 1. In each MCS "trial," a set of random inputs is prepared, a flight simulation is performed incorporating all the inputs, and a result is obtained. Random inputs are generated based on the predetermined distributions of each uncertain parameter, which include aerodynamic model error, actuator model error, errors of inertial characteristics such as mass and moments of inertia, wind conditions, initial conditions, and so on. This process is repeated N times, and the MCS results are obtained as statistical values from the results of the simulation trials, such as the probability of failure and the mean values of target output parameters. Since MCS is a sample survey, the reliability of the MCS result depends only on the number of trials, N, and is independent of the number of input parameters.[18,19] As N increases, the results become more reliable due to the law of large numbers.[20]

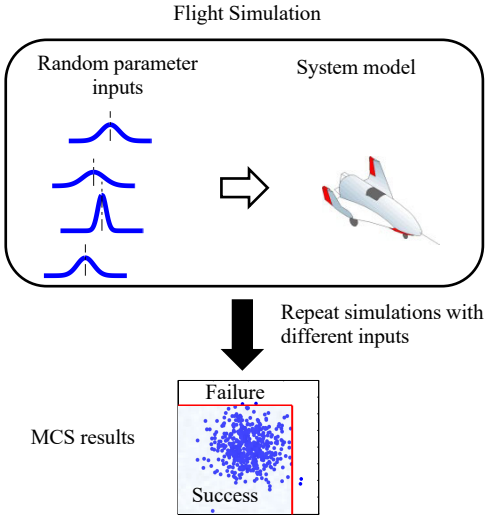

Fig. 1. Monte Carlo simulation.

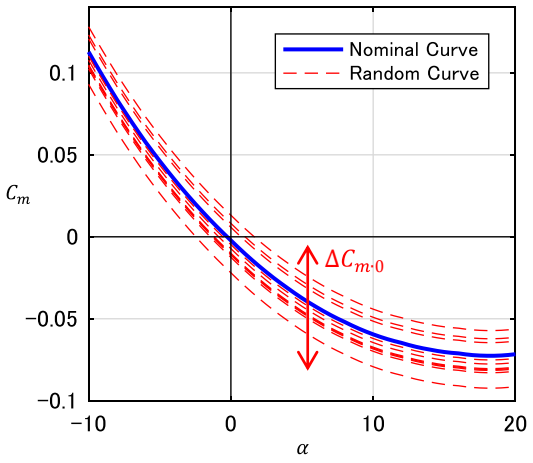

(a) Random bias

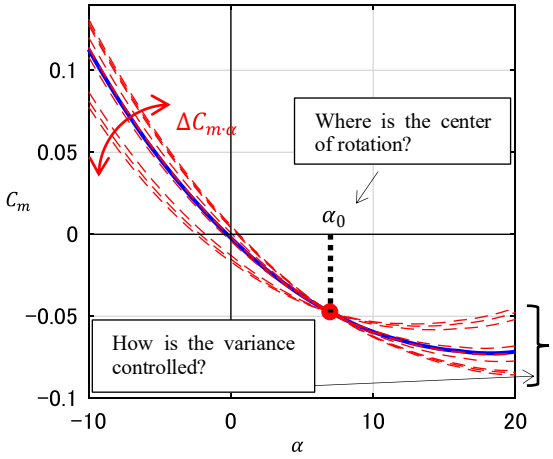

(b) Random derivative

Fig. 2. Example of random generation.

2.2. Random inputs of derivative

There have been some uncertain parameters that have been difficult to incorporate into MCS, including aerodynamic and control derivatives. The uncertainties of bias and derivatives are compared in Fig. 2. An uncertain bias is easy to generate: a random constant value is simply added to the nominal aerodynamic curve as shown in Fig. 2(a). On the other hand, to generate derivative uncertainty, the slope of aerodynamic curve needs to be modified as shown in Fig. 2(b). When random derivatives are generated, there are two issues: 1) where to locate the center of the rotation on the curve, and 2) how to control the variance together with bias uncertainty. Due to these issues, it has been difficult to incorporate derivative uncertainties into MCS inputs appropriately.

3. Random Generation of Derivatives

When aerodynamic parameters including derivatives are estimated from flight data, the estimation error can be obtained as a covariance matrix. The way of considering estimation error can be applied to the problem of random generation of aerodynamic uncertain parameters.

3.1. Parameter estimation

An aerodynamic coefficient, C_A, is expressed as the sum of its nominal value, $C_{A\cdot nom}$, and an uncertain term, ΔC_A:

$$C_A = C_{A\cdot nom} + \Delta C_A \tag{1}$$

The uncertain term, ΔC_A, consists of state variables, uncertain bias and derivatives. For the example shown in Fig. 2, Eq. (1) becomes:

$$C_m = C_{m\cdot nom} + (\Delta C_{m\cdot 0} + \Delta C_{m\cdot\alpha}\cdot\alpha) \tag{2}$$

The uncertain term is expressed as a polynomial function,

$$\Delta C_A = \Delta C_{A\cdot 0} + \Delta C_{A\cdot\alpha}\cdot\alpha + \Delta C_{A\cdot\delta e}\cdot\delta e + \cdots = \boldsymbol{x}^T\cdot\boldsymbol{\beta} \tag{3}$$

where

$$\boldsymbol{x} = \begin{bmatrix} 1 & \alpha & \delta e & \cdots \end{bmatrix}^T$$
$$\boldsymbol{\beta} = \begin{bmatrix} \Delta C_{A\cdot 0} & \Delta C_{A\cdot\alpha} & \Delta C_{A\cdot\delta e} & \cdots \end{bmatrix}^T$$

The vector $\boldsymbol{x}$ includes state variables, and the vector $\boldsymbol{\beta}$ includes uncertain aerodynamic parameters. ΔC_A shows the difference between true C_A and the nominal value, $C_{A\cdot nom}$. Here, $\boldsymbol{x}$ and C_A are assumed to be derived from flight data obtained under various flight conditions. A set of $\boldsymbol{x}$ is expressed as a matrix X as,

$$X = \begin{bmatrix} \boldsymbol{x}_1{}^T \\ \boldsymbol{x}_2{}^T \\ \vdots \\ \boldsymbol{x}_n{}^T \end{bmatrix} = \begin{bmatrix} 1 & \alpha_1 & \delta e_1 & \cdots \\ 1 & \alpha_2 & \delta e_2 & \cdots \\ \vdots & \vdots & \vdots & \vdots \\ 1 & \alpha_n & \delta e_n & \cdots \end{bmatrix} \tag{4}$$

and the corresponding C_A becomes a vector, $\boldsymbol{C}_A = [\, C_{A\cdot 1} \quad C_{A\cdot 2} \quad \cdots \quad C_{A\cdot n}\,]^T$. When the corresponding nominal values, $C_{A\cdot nom}$, are obtained from wind tunnel tests or computational fluid dynamics (CFD) estimates, the uncertain term, $\Delta\boldsymbol{C}_A$, is obtained as the differences between $\boldsymbol{C}_A$ and $C_{A\cdot nom}$. The uncertainty of the aerodynamic coefficient, $\Delta\boldsymbol{C}_A = [\, \Delta C_{A\cdot 1} \quad \Delta C_{A\cdot 2} \quad \cdots]^T$, can then be written in terms of X and $\boldsymbol{\beta}$ as follows:

$$\Delta\boldsymbol{C}_A = X\cdot\boldsymbol{\beta} + \boldsymbol{\varepsilon} \tag{5}$$

where $\boldsymbol{\varepsilon}$ is a residual with a mean value of zero and a variance of σ^2. The unknown parameter, $\boldsymbol{\beta}$, can often be estimated by regression analysis. When it is estimated using the least squares method,[21]

$$\hat{\boldsymbol{\beta}} = \left(X^T X\right)^{-1} X^T\cdot\Delta\boldsymbol{C}_A \tag{6}$$

The estimation error of $\hat{\boldsymbol{\beta}}$ is given by a covariance matrix, Σ, as follows:

$$\Sigma = \sigma^2\left(X^T X\right)^{-1} \tag{7}$$

The unknown parameter, σ^2, can be estimated by,

$$\widehat{\sigma^2} = \left\{\left(\Delta\boldsymbol{C}_A - X\cdot\hat{\boldsymbol{\beta}}\right)^T\left(\Delta\boldsymbol{C}_A - X\cdot\hat{\boldsymbol{\beta}}\right)\right\}\Big/(n-p) \tag{8}$$

where p is the number of independent parameters in Eq. (3). Each diagonal element of Σ is the variance of the corre-

sponding element of $\hat{\boldsymbol{\beta}}$, and the off-diagonal elements are covariances.

Both $\hat{\boldsymbol{\beta}}$ and Σ may be obtained using any estimation method, such as the maximum likelihood method or the Bayesian method.[11] Σ expresses the dispersion of the estimated parameters and corresponds to their uncertainties. The key point for this discussion is that Σ includes covariances in addition to the variance of each parameter, which implies that uncertain parameters are correlated with each other. For example, the dispersion of $\Delta C_{m\cdot 0}$ and that of $\Delta C_{m\cdot\alpha}$ are correlated. In other words, correlated random variables are required for the random generation of derivatives.

3.2. Variance of aerodynamic coefficient

When aerodynamic parameters, $\hat{\boldsymbol{\beta}}$, are varied, the corresponding aerodynamic coefficients, $\widehat{C_A}$, also vary. The relationship between the variance of $\widehat{\Delta C_A}$ and the covariance of $\hat{\boldsymbol{\beta}}$ is obtained as follows. From Eq. (3),

$$\widehat{\Delta C_A} = \boldsymbol{x}^T \cdot \hat{\boldsymbol{\beta}} \tag{9}$$

when the variance of $\widehat{\Delta C_A}$ is V_{CA},

$$\begin{aligned} V_{CA} &= E\left[\widehat{\Delta C_A}^2\right] \\ &= E\left[\left(\boldsymbol{x}^T \cdot \hat{\boldsymbol{\beta}}\right)^2\right] \\ &= E\left[\left(\boldsymbol{x}^T \cdot \hat{\boldsymbol{\beta}}\right)\left(\boldsymbol{x}^T \cdot \hat{\boldsymbol{\beta}}\right)^T\right] \\ &= E\left[\boldsymbol{x}^T\left(\hat{\boldsymbol{\beta}} \cdot \hat{\boldsymbol{\beta}}^T\right)\boldsymbol{x}\right] \\ &= \boldsymbol{x}^T \cdot E\left[\left(\hat{\boldsymbol{\beta}} \cdot \hat{\boldsymbol{\beta}}^T\right)\right] \cdot \boldsymbol{x} \end{aligned} \tag{10}$$

Eq. (10) makes use of the relationship $\left(\boldsymbol{x}^T \cdot \hat{\boldsymbol{\beta}}\right) = \left(\boldsymbol{x}^T \cdot \hat{\boldsymbol{\beta}}\right)^T$ as $\widehat{\Delta C_A}$ is a scalar. Since $E\left[\left(\hat{\boldsymbol{\beta}} \cdot \hat{\boldsymbol{\beta}}^T\right)\right]$ is the covariance matrix, Σ,

$$V_{CA} = \boldsymbol{x}^T \cdot \Sigma \cdot \boldsymbol{x} \tag{11}$$

This equation shows the relationship between the variance of an aerodynamic coefficient and the dispersion of uncertain parameters expressed as Σ. For a certain flight state, $\boldsymbol{x}$, the variance, V_{CA}, is given by Eq. (11). When the aerodynamic uncertainty is given by Σ, the magnitude of V_{CA} depends on $\boldsymbol{x}$.

3.3. Generation of random parameters

In MCS, the uncertain aerodynamic parameters included in $\boldsymbol{\beta}$ need to be generated randomly. In this paper, each element of $\boldsymbol{\beta}$ is assumed to be Gaussian. When generated random parameter vector $\boldsymbol{\beta}$ has Σ, $\boldsymbol{\beta}$ can be generated as follows.[22]

Let $\boldsymbol{u}$ be a random vector in which each element is independent and has a standard normal distribution, $\mathbb{N}(0, 1)$. The converted random vector, $\boldsymbol{r}$, has a correlation matrix of R; the correlation of which is same as that of Σ. Therefore, R is obtained from Σ. When $\boldsymbol{u}$ is converted to $\boldsymbol{r}$ using a constant matrix, P,

$$\boldsymbol{r} = P \cdot \boldsymbol{u} \tag{12}$$

Then, R is obtained by

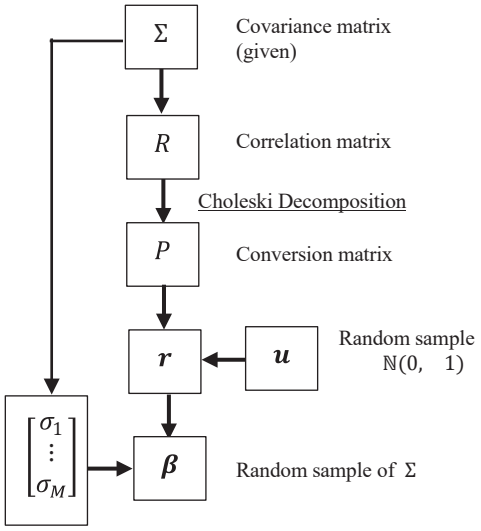

Fig. 3. Procedure for generating $\boldsymbol{\beta}$.

$$\begin{aligned} R &= E\left[\boldsymbol{r} \cdot \boldsymbol{r}^T\right] \\ &= E\left[P\boldsymbol{u} \cdot (P\boldsymbol{u})^T\right] \\ &= P \cdot E\left[\boldsymbol{u} \cdot \boldsymbol{u}^T\right] \cdot P^T \\ &= P \cdot P^T \end{aligned} \tag{13}$$

where, the relationship $E\left[\boldsymbol{u} \cdot \boldsymbol{u}^T\right] = \boldsymbol{I}$ is applied. P can be obtained by Cholesky decomposition of matrix R. After P is obtained, $\boldsymbol{r}$ can be calculated by Eq. (12). Then, $\boldsymbol{r}$ is converted to samples of $\boldsymbol{\beta}$ that have Σ. When the diagonal elements of Σ are $[\,{\sigma_1}^2 \quad \cdots \quad {\sigma_M}^2\,]^T$ and $\boldsymbol{r} = [\,r_1 \quad \cdots \quad r_M\,]^T$, the samples of $\boldsymbol{\beta}$ are obtained by

$$\boldsymbol{\beta} = \left[\,\sigma_1 \cdot r_1 \quad \cdots \quad \sigma_M \cdot r_M\,\right]^T \tag{14}$$

where M is the number of uncertain parameters. The procedure for generating a random sample $\boldsymbol{\beta}$ is shown in Fig. 3.

4. Correlated Aerodynamic Coefficients

Uncertainties of aerodynamic coefficients, ΔC_L and ΔC_D, are often considered to have a strong correlation, and its desirable value, ρ_{req}, should be determined based on aerodynamic investigations of the system. When the value of ρ_{req} is still uncertain, it should be determined as a sort of design parameter in addition to those uncertain input parameters for which there is little information about their ranges. The important thing is to be able to obtain the relationship between the assumed input of MCS and its output. In this case, all of the uncertain parameters included in ΔC_L and ΔC_D should be generated simultaneously. First, the relationship between the correlations of two aerodynamic coefficients and the covariance matrices for uncertain parameters is derived. Then, an example of generating random parameters that incorporate the correlation of ΔC_L and ΔC_D is shown.

4.1. Correlation of two aerodynamic coefficients

The uncertainties of the aerodynamic coefficients can be written as follows:

$$\begin{aligned}\Delta C_L &= \boldsymbol{x}^T \cdot \boldsymbol{\beta}_L \\ \Delta C_D &= \boldsymbol{x}^T \cdot \boldsymbol{\beta}_D\end{aligned} \tag{15}$$

Both $\boldsymbol{\beta}_L$ and $\boldsymbol{\beta}_D$ include uncertain parameters that have uncertain bias and derivatives. The covariance of C_L and C_D is

$$\begin{aligned}V_{LD} &= E[\Delta C_L \cdot \Delta C_D] \\ &= \boldsymbol{x}^T \cdot E\left[\boldsymbol{\beta}_L \cdot \boldsymbol{\beta}_D{}^T\right] \cdot \boldsymbol{x} \\ &= \boldsymbol{x}^T \cdot \Sigma_{LD} \cdot \boldsymbol{x}\end{aligned} \tag{16}$$

where Σ_{LD} is the covariance matrix of $\boldsymbol{\beta}_L$ and $\boldsymbol{\beta}_D$. On the other hand, from Eq. (11), the variances of C_L and C_D are

$$\begin{aligned}V_L &= \boldsymbol{x}^T \cdot \Sigma_L \cdot \boldsymbol{x} \\ V_D &= \boldsymbol{x}^T \cdot \Sigma_D \cdot \boldsymbol{x}\end{aligned} \tag{17}$$

where Σ_L and Σ_D are covariance matrices determined by $\Sigma_L = E\left[\left(\boldsymbol{\beta}_L \cdot \boldsymbol{\beta}_L{}^T\right)\right]$ and $\Sigma_D = E\left[\left(\boldsymbol{\beta}_D \cdot \boldsymbol{\beta}_D{}^T\right)\right]$, respectively. Then, correlation ρ_{LD} between the aerodynamic coefficients C_L and C_D can be calculated by

$$\rho_{LD} = V_{LD} / \left(\sqrt{V_L} \cdot \sqrt{V_D}\right) \tag{18}$$

ρ_{LD} is a correlation coefficient for a certain flight condition of $\boldsymbol{x}$ which includes flight parameters such as angle-of-attack α, and control parameters such as elevator control angle, δe. That is, ρ_{LD} varies depending on $\boldsymbol{x}$, and so it is usually impossible for ρ_{LD} to be expressed by a fixed given value of ρ_{req}. Nevertheless, ρ_{LD} can be adjusted to become close to ρ_{req} using numerical optimization to tune the elements of Σ_{LD}.

4.2. Example for adjusting Σ_{LD}

In this example, the uncertainties are given as follows:

$$\begin{aligned}\Delta C_L &= \Delta C_{L\cdot 0} + \Delta C_{L\cdot\alpha} \cdot \alpha \\ \Delta C_D &= \Delta C_{D\cdot 0}\end{aligned} \tag{19}$$

Here, the uncertainty ΔC_D consists of a bias term only for simplicity. In this case the state variable is

$$\boldsymbol{x} = \begin{bmatrix} 1 & \alpha \end{bmatrix}^T \tag{20}$$

and the uncertain vectors are

$$\begin{aligned}\boldsymbol{\beta}_L &= \begin{bmatrix} \Delta C_{L\cdot 0} & \Delta C_{L\cdot\alpha} \end{bmatrix}^T \\ \boldsymbol{\beta}_D &= \begin{bmatrix} \Delta C_{D\cdot 0} & 0 \end{bmatrix}^T\end{aligned} \tag{21}$$

Suppose the covariance matrices are given as

$$\begin{aligned}\Sigma_L &= \begin{bmatrix} {\sigma_{L\cdot 0}}^2 & \rho_L \cdot \sigma_{L\cdot 0}\sigma_{L\cdot\alpha} \\ \rho_L \cdot \sigma_{L\cdot 0}\sigma_{L\cdot\alpha} & {\sigma_{L\cdot\alpha}}^2 \end{bmatrix} \\ \Sigma_D &= \begin{bmatrix} {\sigma_{D\cdot 0}}^2 & 0 \\ 0 & 0 \end{bmatrix}\end{aligned} \tag{22}$$

The covariance matrix Σ_{LD} is obtained from Eq. (16):

$$\begin{aligned}\Sigma_{LD} &= E\left[\boldsymbol{\beta}_L \cdot \boldsymbol{\beta}_D{}^T\right] \\ &= \begin{bmatrix} E[\Delta C_{L\cdot 0} \cdot \Delta C_{D\cdot 0}] & 0 \\ E[\Delta C_{L\cdot\alpha} \cdot \Delta C_{D\cdot 0}] & 0 \end{bmatrix} \\ &= \begin{bmatrix} v_{LD\cdot 0} & 0 \\ v_{LD\cdot\alpha} & 0 \end{bmatrix}\end{aligned} \tag{23}$$

where $v_{LD\cdot 0} = E[\Delta C_{L\cdot 0} \cdot \Delta C_{D\cdot 0}]$ and $v_{LD\cdot\alpha} = E[\Delta C_{L\cdot\alpha} \cdot \Delta C_{D\cdot 0}]$, and these covariances are unknown parameters to be determined.

Then, the covariance V_{LD} and variances of the aerodynamic coefficients V_L and V_D are obtained by Eq. (16) and Eq. (17). The correlation between C_L and C_D is obtained from Eq. (18) as

$$\rho_{LD} = \frac{v_{LD\cdot 0} + v_{LD\cdot\alpha} \cdot \alpha}{\sqrt{\boldsymbol{x}^T \cdot \Sigma_L \cdot \boldsymbol{x}}\sqrt{\boldsymbol{x}^T \cdot \Sigma_D \cdot \boldsymbol{x}}} \tag{24}$$

While it is desirable that ρ_{LD} can become equal to the requirement, ρ_{req}, it is impossible because ρ_{LD} is a function of α. Even so, ρ_{LD} can be made to be close to ρ_{req} using numerical optimization. Several cost functions to be minimized can be considered for the optimization, and one example is shown as follows. The target range of α is divided into n values $[\,\alpha_1 \quad \cdots \quad \alpha_n\,]$ at equal intervals of $\Delta\alpha$. Then, the cost function, $J(\Sigma_{LD})$, is determined as

$$J(\Sigma_{LD}) = \sum_{i=1}^{n} \left\{\rho_{LD}(\Sigma_{LD}, \alpha_i) - \rho_{req}\right\}^2 \tag{25}$$

After J is minimized by an optimization algorithm such as the Downhill SIMPLEX method,[12] the optimized Σ_{LD} can be obtained. That is, optimized values of $v_{LD\cdot 0}$ and $v_{LD\cdot\alpha}$ are obtained in this example.

Once Σ_{LD} is determined, uncertain parameters $\boldsymbol{\beta}_L$ and $\boldsymbol{\beta}_D$ can be generated. $\boldsymbol{\beta}$ and Σ can be determined as follows:

$$\boldsymbol{\beta} = \begin{bmatrix} \boldsymbol{\beta}_L{}^T & \boldsymbol{\beta}_D{}^T \end{bmatrix}^T \tag{26}$$

$$\Sigma = \begin{bmatrix} \Sigma_L & \Sigma_{LD} \\ \Sigma_{LD}{}^T & \Sigma_D \end{bmatrix} \tag{27}$$

Then, $\boldsymbol{\beta}$ can be generated by the procedure shown in Fig. 3. Since $\boldsymbol{\beta}_D$ includes only one parameter in this example, $\boldsymbol{\beta}$ and Σ can be reduced to a (3×1) vector and a (3×3) matrix, respectively.

4.3. Numerical example

The covariance matrix Σ_{LD} can be adjusted so that ρ_{LD} becomes close to ρ_{req}. In this example, Σ_L and Σ_D are given as

$$\begin{aligned}\Sigma_L &= \begin{bmatrix} 0.0583^2 & -0.75 \cdot 0.0583 \cdot 0.00293 \\ & 0.00293^2 \end{bmatrix} \\ \Sigma_D &= \begin{bmatrix} 0.03^2 & 0 \\ & 0 \end{bmatrix}\end{aligned} \tag{28}$$

As the covariance matrix is symmetric, the lower triangular elements are dropped to keep the expression uncluttered. Then, Σ becomes:

$$\Sigma = \begin{bmatrix} 0.0583^2 & -0.75 \cdot 0.0583 \cdot 0.00293 & v_{LD\cdot 0} \\ & 0.00293^2 & v_{LD\cdot\alpha} \\ & & 0.03^2 \end{bmatrix} \tag{29}$$

The unknown covariances $v_{LD\cdot 0}$ and $v_{LD\cdot\alpha}$ are determined by minimizing the cost function, J, in Eq. (25). In this example, J is minimized with ρ_{req} given as

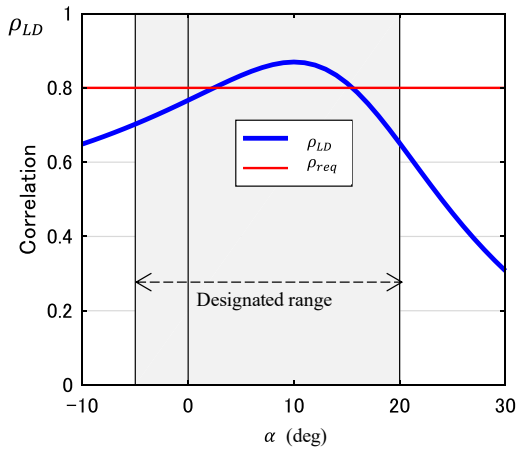

Fig. 4. Correlation between C_L and C_D.

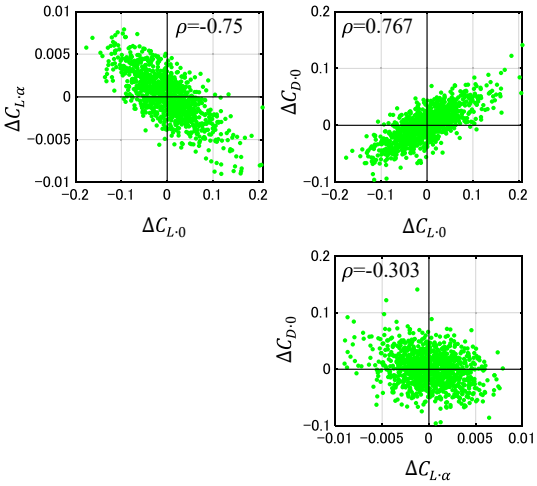

Fig. 5. Distributions of 1,000 uncertain variables generated.

$$\rho_{req} = 0.8 \tag{30}$$

When the range of α is $[-5, 20]$ deg and $\Delta\alpha = 0.1$ deg, the optimized results are

$$\begin{aligned} v_{LD\cdot 0} &= 0.767 \cdot 0.0583 \cdot 0.03 \\ v_{LD\cdot\alpha} &= -0.303 \cdot 0.00293 \cdot 0.03 \end{aligned} \tag{31}$$

As the result of the optimization, the correlation coefficient, ρ_{LD}, that is shown in Fig. 4 is obtained from Eq. (24). Although ρ_{LD} is a function of α, it becomes close to ρ_{req} in the designated range of α.

Once Σ of Eq. (29) is determined, $\boldsymbol{\beta}$, namely $\Delta C_{L\cdot 0}$, $\Delta C_{L\cdot\alpha}$ and $\Delta C_{D\cdot 0}$, can be generated simultaneously using the procedure stipulated in Fig. 3. The generated uncertain samples are shown in Fig. 5. The corresponding uncertain samples are shown in Fig. 6. The range of variation of ΔC_L depends on the value of α, while that of ΔC_D stays constant corresponding to Eq. (22). A cross plot of ΔC_L and ΔC_D is shown in Fig. 7. ΔC_L varies depending on α, while ΔC_D stays constant for each sample of the aerodynamic curve. The uncertain parts, ΔC_L and ΔC_D, are added to the corresponding nominal aerodynamic curves in Fig. 8.

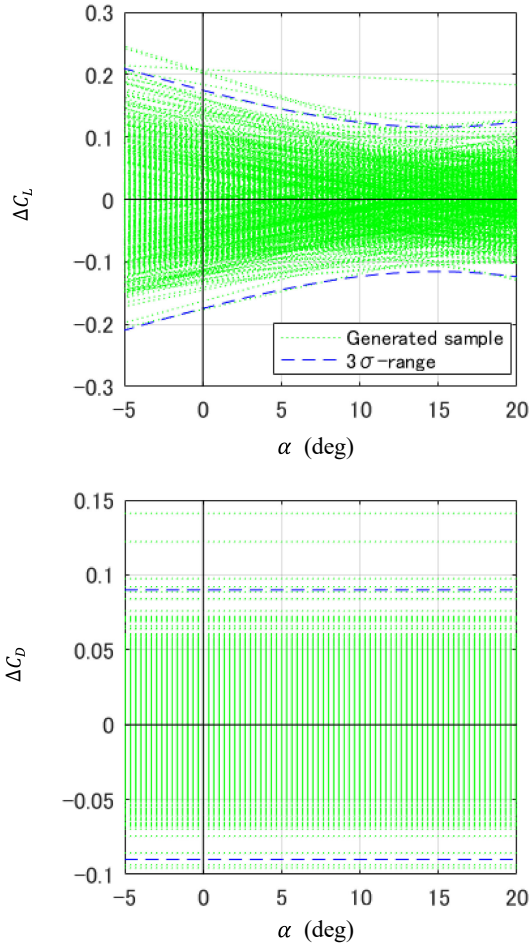

Fig. 6. Uncertainties of ΔC_L and ΔC_D.

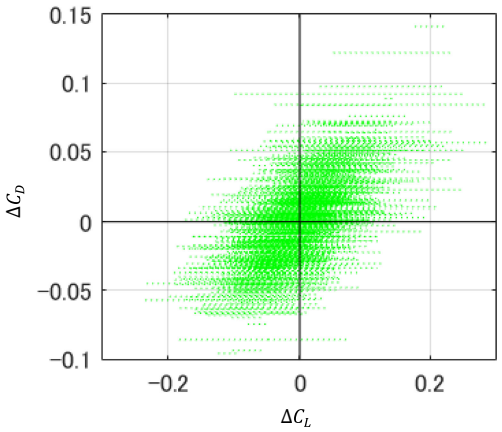

Fig. 7. Relationship between ΔC_L and ΔC_D.

5. Application to Flight System

In this section, the application of the method presented is demonstrated by incorporating derivative uncertainties into the MCS evaluation of a flight system. The flight system in this demonstration is the Automatic Landing FLight EXperiment (ALFLEX),[1,23–25] which was conducted in 1996. First, the ALFLEX system is briefly introduced and the conditions of the flight simulation are specified. Then, an uncertain ran-

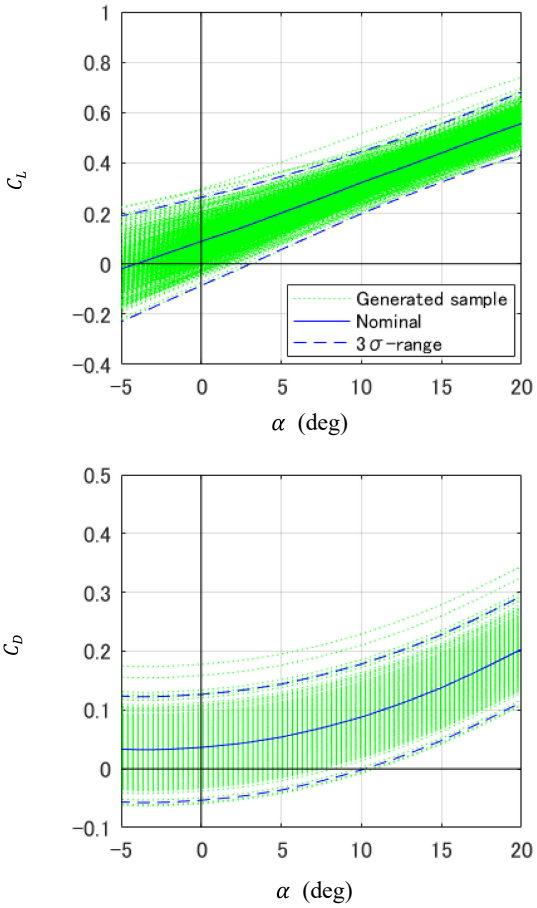

Fig. 8. Uncertainties of C_L and C_D.

Fig. 9. ALFLEX vehicle in flight.

dom model for C_m including uncertain derivatives is constructed. Finally, MCS is conducted to evaluate the influence of the derivative uncertainties.

5.1. ALFLEX

The ALFLEX flight experiment campaign was carried out at Woomera Airfield in Australia in order to establish automatic landing technologies for a future re-entry vehicle. A total of 13 automatic landing experiments were successfully conducted. Figure 9 shows the ALFLEX vehicle in flight, and Fig. 10 shows an orthographic projection of the vehicle.

The flight profile for the experiment is shown in Fig. 11. At first, the vehicle is flown at a level flight suspended underneath a helicopter by a single cable. The vehicle is then released into free flight about 2,700 m from the runway, and

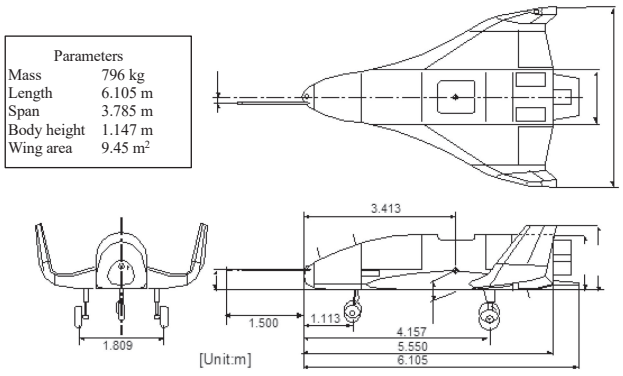

Fig. 10. Three views of ALFLEX vehicle.

guided to approach the runway and land using an onboard guidance and navigation computer. Prior to the experiment, flight simulations using MCS were performed to evaluate flight safety, vehicle performance, and the probability of success.

5.2. Condition for MCS

Flight simulations were performed from vehicle release to touchdown on the runway. The MCS incorporated more than 100 uncertain input parameters of the categories shown in Fig. 12. The distributions and ranges of all input parameters are given in the appendix of a study by Motoda.[26] The uncertainty of C_m is included in the "aerodynamic model error," and at that time, it excluded derivative uncertainty. Flight performance was evaluated by the conditions at touchdown and the vehicle's stability assessed by its attitude in flight.

5.3. C_m random model

The nominal model, $C_{m\cdot nom}$, which includes no uncertainty, is shown in Fig. 13 with the functions of α and δe. The aerodynamic model including uncertainty is the following expression for C_m

$$C_m = C_{m\cdot nom} + \Delta C_m(\alpha, \delta e) \tag{32}$$

where ΔC_m is the uncertain term including bias and derivative uncertainties:

$$\Delta C_m(\alpha, \delta e) = \Delta C_{m\cdot 0} + \Delta C_{m\cdot\alpha} \cdot \alpha + \Delta C_{m\cdot\delta e} \cdot \delta e \tag{33}$$

Equation (33) can be written using $\boldsymbol{x} = [\,1 \quad \alpha \quad \delta e\,]^T$ and $\boldsymbol{\beta} = [\,\Delta C_{m\cdot 0} \quad \Delta C_{m\cdot\alpha} \quad \Delta C_{m\cdot\delta e}\,]^T$ as

$$\Delta C_m(\alpha, \delta e) = \boldsymbol{x}^T \cdot \boldsymbol{\beta} \tag{34}$$

From Eq. (11), the variance of ΔC_m (or C_m) can be obtained by

$$V_{cm} = \boldsymbol{x}^T \cdot \Sigma \cdot \boldsymbol{x} \tag{35}$$

where $\Sigma = E\left[\boldsymbol{\beta} \cdot \boldsymbol{\beta}^T\right]$ and its elements are

$$\Sigma = \begin{bmatrix} {\sigma_0}^2 & \rho_{0\alpha} \cdot \sigma_0\sigma_\alpha & \rho_{0e} \cdot \sigma_0\sigma_e \\ & {\sigma_\alpha}^2 & \rho_{\alpha e} \cdot \sigma_\alpha\sigma_e \\ & & {\sigma_e}^2 \end{bmatrix} \tag{36}$$

The diagonal elements are the variances of each element of $\boldsymbol{\beta}$. The off-diagonal elements are the covariances of the two corresponding elements of $\boldsymbol{\beta}$, and $\rho_{0\alpha}$, ρ_{0e} and $\rho_{\alpha e}$ are correlation coefficients. The variances are

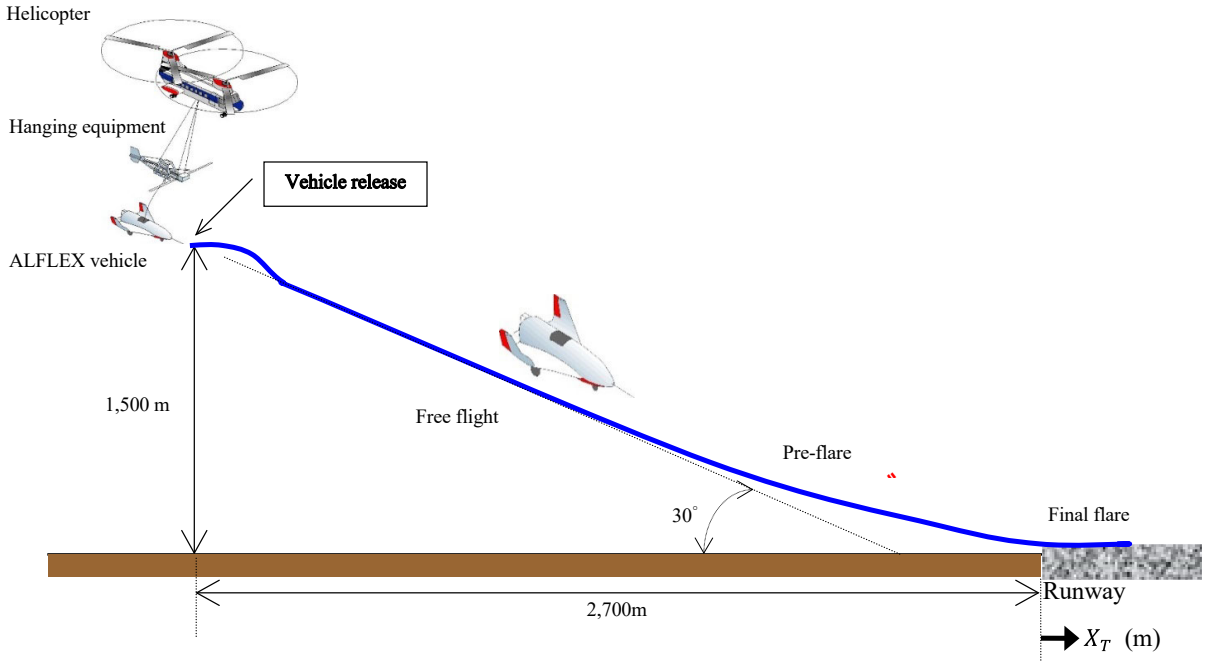

Fig. 11. ALFLEX flight path.

Vehicle Model Error

- Inertial characteristics error
- Aerodynamic model error
- Actuator model error

Sensor Measurement Error

- Inertial measurement unit (IMU)
- Air data sensor (ADS)
- Microwave landing system (MLS)
- Rader altimeter (RA)

Environmental conditions

- Steady wind
- Gravitational acceleration
- Atmospheric temperature
- Atmospheric pressure

Initial conditions

- State variables at vehicle release
- Navigation error

Random Time Series

- Gust
- Sensor output

Fig. 12. Uncertain parameters.

$$\begin{aligned} {\sigma_0}^2 &= \left(6.67 \times 10^{-3}\right)^2 \\ {\sigma_\alpha}^2 &= \left(7.03 \times 10^{-4}\right)^2 \\ {\sigma_e}^2 &= \left(3.49 \times 10^{-4}\right)^2 \end{aligned} \tag{37}$$

However, the correlation coefficients are unknown and Σ is undetermined. Properly, Σ including correlation coefficients should have been determined for the preflight evaluation

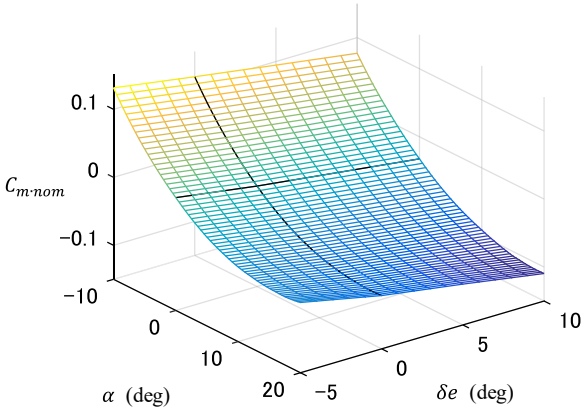

Fig. 13. C_m nominal model.

by investigating the vehicle's aerodynamic characteristics through wind tunnel test results, etc. However, since the importance of the covariances in Σ for modelling uncertain parameters has not previously been recognized, it is unlikely that their values could have been estimated.

Notwithstanding, correlation coefficients must be determined to incorporate derivative uncertainties into the uncertain aerodynamic model. If each element of $\boldsymbol{\beta}$ varies independently, that is, if all correlation coefficients are set to zero, the variance of C_m might become excessively large and unrealistic. Correlation coefficients need to be adjusted to set the variance of C_m within a reasonable range. Although there is no correct solution for the correlation coefficients because the true values are unknown, rational values should be determined as a sort of design parameter. While there are a number of ways in which the correlations could be adjusted, in this example numerical optimization was applied as explained in the following section.

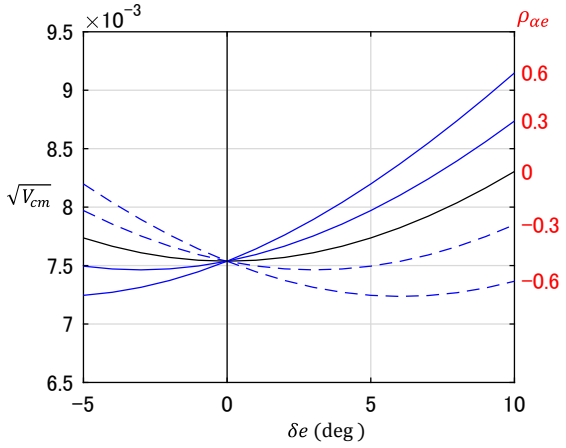

(a) Influence of $\rho_{\alpha e}$

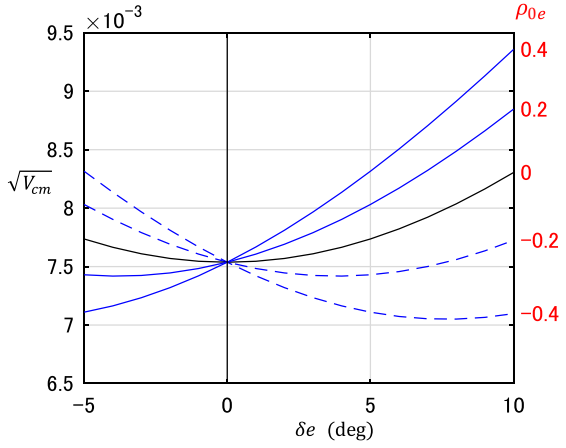

(b) Influence of ρ_{0e}

Fig. 14. Influence on C_m variation at $\alpha = 5°$.

5.4. Correlation setting

Equation (35) is expanded with respect to δe as

$$V_{cm} = {\sigma_e}^2 \cdot \delta e^2 + 2\{(\rho_{\alpha e} \cdot \sigma_\alpha \sigma_e) \cdot \alpha + (\rho_{0e} \cdot \sigma_0 \sigma_e)\} \cdot \delta e + \{{\sigma_\alpha}^2 \cdot \alpha + 2(\rho_{0\alpha} \cdot \rho_0 \rho_\alpha) + {\sigma_0}^2\} \tag{38}$$

The variance, V_{cm}, should be reasonable for the ranges of $\boldsymbol{x}$, namely α and δe, to be considered. First, it is assumed that α is fixed and V_{cm} is a function of δe. Then, V_{cm} takes its minimum value when δe becomes

$$\delta e_{min} = -\{(\rho_{\alpha e} \cdot \sigma_\alpha \sigma_e)\alpha + (\rho_{0e} \cdot \sigma_0 \sigma_e)\}/{\sigma_e}^2 \tag{39}$$

The correlation coefficients that affect δe_{min} are $\rho_{\alpha e}$ and ρ_{0e}. First, the influence of $\rho_{\alpha e}$ is investigated and is illustrated in Fig. 14(a) for $\rho_{0\alpha} = \rho_{0e} = 0$ and $\alpha = 5°$. The vertical axis shows the standard deviation of C_m; that is, the $\sqrt{V_{cm}}$ obtained from Eq. (38). As $\rho_{\alpha e}$ increases, $\sqrt{V_{cm}}$ also increases for $\delta e > 0°$. In addition, Eq. (39) indicates that δe_{min} varies when $\rho_{\alpha e}$ has a non-zero value and α changes. This means that the V_{cm} curve is affected by changes in both α and δe. To avoid a complicated the model, $\rho_{\alpha e}$ is set to zero, since no information about correlations is available.

On the other hand, the influence of ρ_{0e} is shown in Fig. 14(b) for $\rho_{0\alpha} = \rho_{\alpha e} = 0$. $\sqrt{V_{cm}}$ also increases as ρ_{0e} increases for $\delta e > 0°$. However, unlike $\rho_{\alpha e}$, δe_{min} can be fixed when $\rho_{\alpha e} = 0$ and ρ_{0e} is fixed. Therefore, the fixed value of ρ_{0e} determines δe_{min}, which is the elevator angle that gives minimum V_{cm}. The appropriate value of ρ_{0e} depends both on the flight system and on the design concept. For example, if the elevator deflection δe is symmetric about $\delta e = 0$ in flight, then $\rho_{0e} = 0$ might be appropriate because $\sqrt{V_{cm}}$ also becomes symmetric about $\delta e = 0$. Alternatively, if the vehicle flies with a trim angle of δe_{trim} for most of the flight duration, then it may be appropriate to adjust ρ_{0e} so that $\delta e_{min} = \delta e_{trim}$ because the flight system is unlikely to be affected by uncertainty during trimmed flight, as compared to transitional flight between trimmed states. Since the objective of this example is to show how to determine correlations using numerical optimization, ρ_{0e} was set to be zero for simplicity.

After setting the correlation $\rho_{\alpha e} = \rho_{0e} = 0$, the remaining $\rho_{0\alpha}$ needed to be determined by numerical optimization as follows. First, the ranges of α and δe were determined considering the flight conditions, and were divided at regular intervals respectively as follows:

$$\begin{aligned} \{\alpha\} &= \{\, \alpha_1 \quad \cdots \quad \alpha_i \quad \cdots \quad \alpha_n \,\} \\ \{\delta e\} &= \{\, \delta e_1 \quad \cdots \quad \delta e_j \quad \cdots \quad \delta e_m \,\} \end{aligned} \tag{40}$$

Though there would be several ways to determine a cost function for the optimization, the variation of $\sqrt{V_{cm}}$ in the determined ranges of α and δe is minimized in this example. That is, the variance of $\sqrt{V_{cm}}$ is minimized and the cost function J is determined as

$$J(\rho_{0\alpha}) = \frac{1}{n \cdot m} \sum_{i=1}^{n} \sum_{j=1}^{m} \left\{ \sqrt{V_{cm}(\rho_{0\alpha}, \alpha_i, \delta e_j)} - S_{mean}(\rho_{0\alpha}) \right\}^2 \tag{41}$$

where

$$S_{mean}(\rho_{0\alpha}) = \frac{1}{n \cdot m} \sum_{i=1}^{n} \sum_{j=1}^{m} \sqrt{V_{cm}(\rho_{0\alpha}, \alpha_i, \delta e_j)} \tag{42}$$

S_{mean} indicates the mean value of the standard deviation $\sqrt{V_{cm}}$ in the designated ranges of α and δe, and the righthand side of Eq. (41) shows the variance of $\sqrt{V_{cm}}$. When all $\sqrt{V_{cm}(\rho_{0\alpha}, \alpha_i, \delta e_j)}$, $(i = 1, \cdots, n,\ \ j = 1, \cdots, m)$ have the same value, J becomes its minimum value of zero.

The ranges of α and δe for a nominal flight in which no uncertainties are incorporated are shown in Fig. 15. The ranges are determined covering the nominal ranges,

$$\alpha\text{: } [\, -5 \quad 20 \,] \text{ and } \delta e\text{: } [\, -5 \quad 10 \,]$$

Then, J was minimized using the Downhill-SIMPLEX method and $\rho_{0\alpha}$ obtained as

$$\rho_{0\alpha} = -0.45 \tag{43}$$

The optimized range of $\sqrt{V_{cm}}$ is shown in Fig. 16. Since V_{cm} is symmetric about $\delta e = 0°$, the value of $\sqrt{V_{cm}}$ exists within the gray zone.

The influence of $\rho_{0\alpha}$ for $\rho_{\alpha e} = \rho_{0e} = 0$ obtained from Eq. (38) is illustrated in Fig. 17. The solid line shows the op-

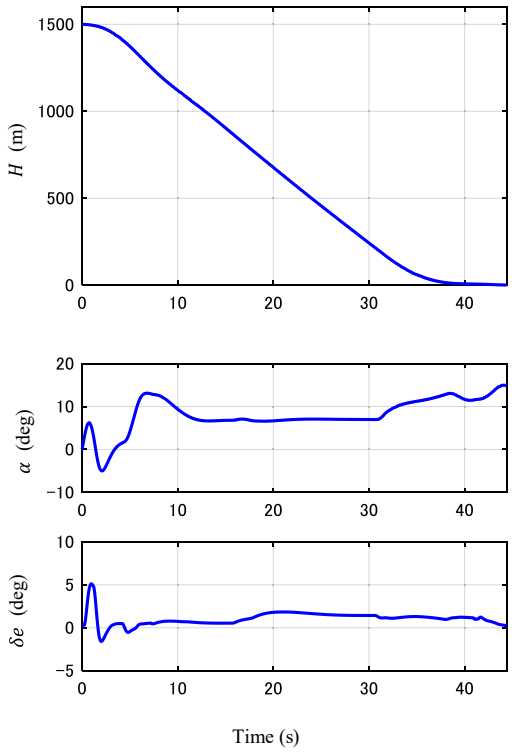

Fig. 15. Time history of a nominal flight.

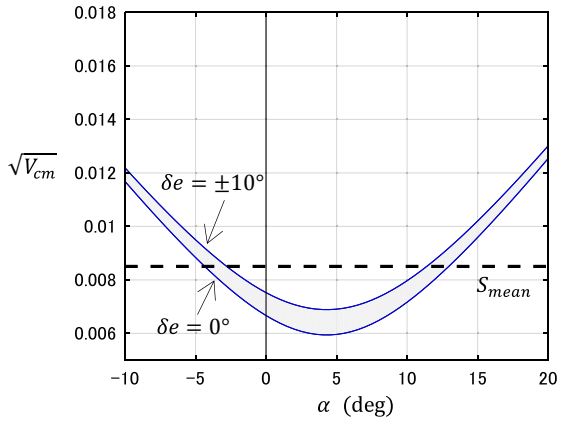

Fig. 16. Optimized standard deviation of C_m.

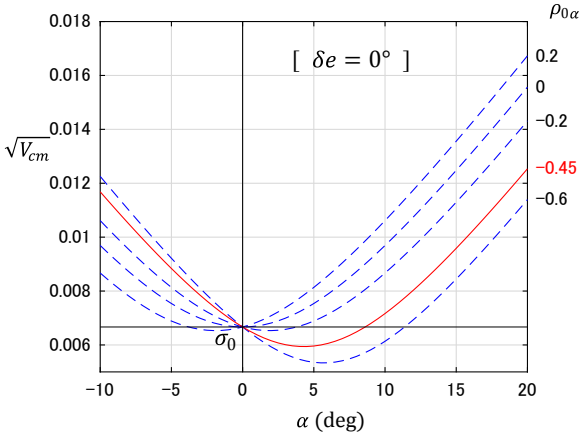

Fig. 17. Influence of $\rho_{0\alpha}$ on $\sqrt{V_{cm}}$.

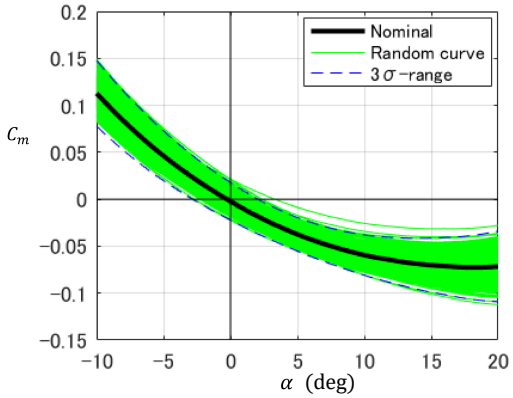

(a) Derivative uncertainty included [Input A]

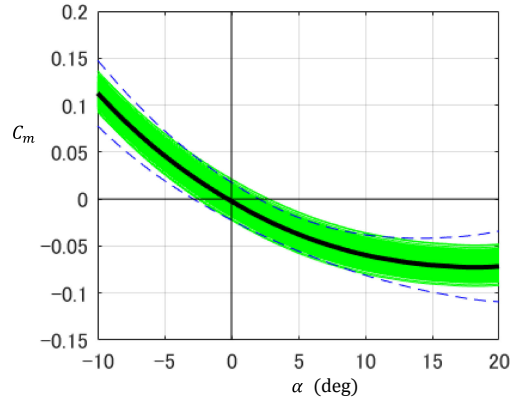

(b) Bias uncertainty only [Input B]

Fig. 18. 1,000 samples of generated C_m ($\delta e = 0$).

timized value. As $\rho_{0\alpha}$ increases, the variation of C_m becomes large for $\alpha > 0$. When $\rho_{0\alpha} = 0$, or when uncertain parameters are generated independently, the variation is considerably larger than that of the optimized one. On the other hand, if derivative uncertainties are excluded and only $\Delta C_{m\cdot 0}$ is included, the standard deviation $\sqrt{V_{cm}}$ has a constant value of σ_0. The optimized solid line is below σ_0 when α has a positive low value. This means that the variation of C_m including derivative uncertainties is smaller than that excluding them.

Random samples of the uncertain parameters are generated and plotted as a C_m–α curve in Fig. 18. Derivative uncertainties, $\Delta C_{m\cdot\alpha}$ and $\Delta C_{m\cdot\delta e}$, as well as $\Delta C_{m\cdot 0}$, are included in Fig. 18(a) as curves tagged with [Input A]. The "3σ-range" shown by the broken line indicates the $3\sqrt{V_m}$ obtained from Eq. (38). In contrast, only $\Delta C_{m\cdot 0}$ is included in Fig. 18(b) as curves tagged with [Input B]. The "3σ-range" between the broken lines is given for [Input A], and the same broken lines are shown in Fig. 18(b) to make the difference between [Input A] and [Input B] clear. [Input A] corresponds to the solid line of $\rho_{0\alpha} = -0.45$ and [Input B] corresponds to the horizontal line of $\sqrt{V_{cm}} = \sigma_0$ in Fig. 17.

5.5. MCS results

The influence of derivative uncertainties is confirmed by comparing MCS results computed using the two sets of inputs, [Input A] and [Input B], in Fig. 18. MCS was per-

formed using the more than 100 uncertain input parameters shown in Fig. 12. Among the uncertainties, the two sets of random curves shown in Fig. 18(a) and (b) were used as aerodynamic model errors of C_m, while the other uncertain parameters were identical.

The MCS results are shown in Table 1, which gives the number of simulation results that failed to meet the requirements (namely, failure cases). The evaluated parameters are mainly touchdown states such as vertical speed, touchdown distance from the runway threshold, and stability during flight which evaluates whether or not the vehicle can reach the runway successfully. The total number of failures in [Input A] is 56 and is much greater than the 30 of [Input B]. Each result (probability of failure) indicates the sample value taken randomly from the corresponding population. Therefore, the range in which the true value is included should be estimated by deriving the confidence intervals in order to compare the results of [Input A] and [Input B].[10,18,19] The confidence intervals of the probability of failure are $[4.4, 6.9](\%)$ for [Input A] and $[2.2, 4.0](\%)$ for [Input B] with a confidence level of 90%. This difference is statistically significant because the confidence intervals are not crossover. An example of touchdown states of $V_{g\cdot T}$ and $\dot{Z}_T$ are illustrated in Fig. 19. The failure cases are indicated by "×" marks. Although the MCS-calculated probabilities of failure are much different, the trends of the failure cases in the graphs appear similar.

Table 1. MCS results: Numbers of simulation results that exceeded each requirement.

Requirement	[Input A]	[Input B]
Unstable	0	0
[Touchdown state↓]		
X_T position	5	2
Y_T position	0	0
$\dot{Z}_T$	53	29
$\beta_{g\cdot T}$	0	0
Θ_T	0	0
Φ_T	0	0
$V_{g\cdot T}$	6	3
Total	56	30

(Total number of simulations: 1,000)

The derivative uncertainties that were found to have significant influences on the MCS results are specific to the ALFLEX flight system studied in this example, and they may have little influence in other flight systems. Whatever the identified derivative uncertainties may be, the important thing is that they should be incorporated into MCS so that the results reflect their influences.

6. Conclusion

MCS has become an important tool for preflight evaluation in the development of aerospace vehicles. Various uncertain parameters can be incorporated into MCS evaluation, and aerodynamic uncertainties are important part of the inputs that affect flight motion. Specifically, variations of aerodynamic and control derivatives, such as $C_{m\cdot\alpha}$ and $C_{m\cdot\delta e}$, are known to be influential parameters on flight control. However, such variations of derivatives have been difficult to incorporate into MCS evaluation hitherto, and so previous MCS results have excluded the influences of derivative variations. In this paper, a method of generating random inputs of an aerodynamic model incorporating derivative uncertainties is presented. In this method, random aerodynamic curves are generated using correlations of derivatives and bias uncertainties, and the variance of the generated aerodynamic coefficient can be adjusted by the correlation coefficients. When inputting uncertainties of aerodynamic coefficients, such as C_L and C_D, includes a degree of correlation, random samples of the corresponding aerodynamic curves can also be generated simultaneously considering all correlations of related derivatives and biases. The influence of derivative uncertainties in MCS was demonstrated by investigating an automatic landing flight system. The results showed that derivative uncertainties are quite influential, and implies that including derivative uncertainties in MCS is important. By incorporating the approach presented here, MCS is expected to become an even more reliable preflight evaluation tool.

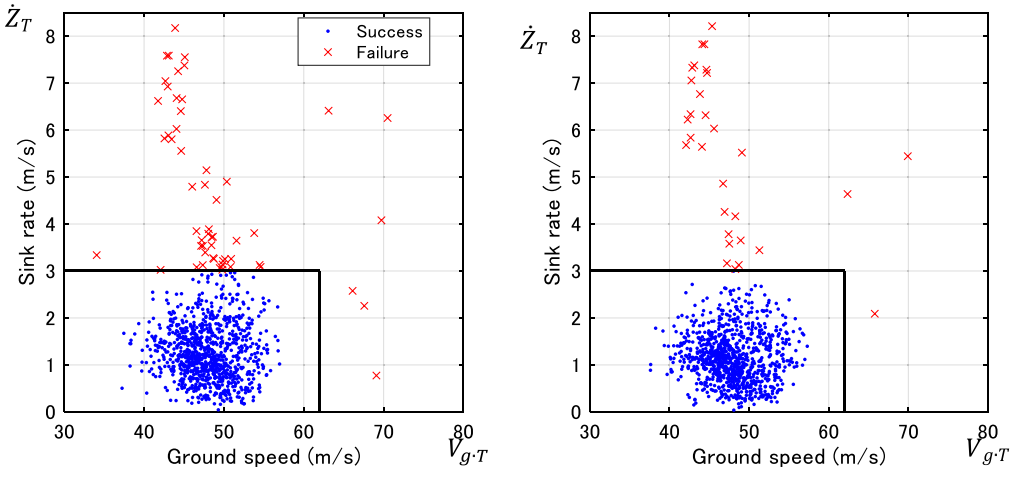

(a) Result for [Input A]

(b) Result for [Input B]

Fig. 19. Touchdown states of 1,000 MCS results.

References

1) Motoda, T., Miyazawa, Y., Ishikawa, K., and Izumi, T.: Automatic Landing Flight Experiment Flight Simulation Analysis and Flight Testing, *J. Spacecr. Rockets*, **36**, 4 (1999), pp. 554–560. https://doi.org/10.2514/3.27199
2) Hamada, Y., Ninomiya, T., Katayama, Y., Shinomiya, Y., Matsumoto, K., Yamamoto, M., Sawai, S., Ueno, S., and Hayashi, K.: Feasibility Study for Precise Lunar Landing Using SELENE-B Lander Configuration, JAXA-RR-05-013E, 2005. http://id.nii.ac.jp/1696/00002280/
3) Ninomiya, T., Suzuki, H., and Tsukamoto, T.: Evaluation of Guidance and Control Systems of a Balloon-Launched Drop Test Vehicle, *J. Spacecr. Rockets*, **43**, 6 (2006), pp. 1423–1425. https://doi.org/10.2514/1.23265
4) Ninomiya, T., Suzuki, H., and Kawaguchi, J.: Dynamic Inversion Controller Design for Balloon-Launched Supersonic Aircraft, *Trans. Jpn. Soc. Aeronaut. Space Sci.*, **61**, 6 (2018), pp. 248–257. https://doi.org/10.2322/tjsass.61.248
5) Schubert, W. M. and Stengel, R. F.: Parallel Synthesis of Robust Control Systems, *IEEE Trans. Control Syst. Technol.*, **6**, 6 (1998), pp. 701–706. https://doi.org/10.1109/87.726531
6) Motoda, T. and Miyazawa, Y.: Identification of Influential Uncertainties in Monte Carlo Analysis, *J. Spacecr. Rockets*, **39**, 4 (2002), pp. 615–623. https://doi.org/10.2514/2.3851
7) Motoda, T.: Simplified Approach to Identifying Influential Uncertainties in Monte Carlo Analysis, *J. Spacecr. Rockets*, **41**, 6 (2004), pp. 1071–1075. https://doi.org/10.2514/1.10265
8) Restrepo, C. I. and Hurtado, J. E.: Tool for Rapid Analysis of Monte Carlo Simulations, *J. Spacecr. Rockets*, **51**, 5 (2014), pp. 1564–1575. https://doi.org/10.2514/1.A32679
9) Motoda, T.: Quick Detection of Influential Inputs in Monte Carlo Simulation, *J. Aerosp. Inf. Syst.*, **19**, 2 (2022), pp. 113–123. https://doi.org/10.2514/1.I010926
10) Conover, W. J.: *Practical Nonparametric Statistics*, 3rd edition, John Wiley & Sons, Inc., New York, 1999, pp. 30–31, 81–84, 131–133, 188–190. ISBN 9780471160687
11) Bishop, C. M.: *Pattern Recognition and Machine Learning*, Springer, New York, 2006, pp. 120–127, 137–173. ISBN 9780387310732
12) Press, W. H., Teukolsky, S. A., Vetterling, W. T., and Flannery, B. P.: *Numerical Recipes in C*, 2nd edition, Cambridge Univ. Press, New York, 1992, pp. 408–412, 620–628. ISBN 0521431085
13) Stephens, M. A.: The Goodness-of-fit Statistic V_N: Distribution and Significance Points, *Biometrika*, **52**, 3-4 (1965), pp. 309–321.
14) Devore, J. L.: *Probability and Statistics for Engineering and Sciences*, 9th edition, Metric Version, Cengage Learning, Boston, 2016, pp. 326–330. ISBN 9781305251809
15) Marrison, C. I. and Stengel, R. F.: Design of Robust Control Systems for Hypersonic Aircraft, *J. Guid. Control Dynam.*, **21**, 1 (1998), pp. 58–63. https://doi.org/10.2514/2.4197
16) Miyazawa, Y. and Motoda, T.: Stochastic Parameter Tuning Applied to Space Vehicle Flight Control Design, *J. Guid. Control Dynam.*, **24**, 3 (2001), pp. 597–604. https://doi.org/10.2514/2.4751
17) Motoda, T., Stengel, R. F., and Miyazawa, Y.: Robust Control System Design Using Simulated Annealing, *J. Guid. Control Dynam.*, **25**, 2 (2002), pp. 267–274. https://doi.org/10.2514/2.4878
18) Stengel, R. F.: *Flight Dynamics*, Princeton University Press, New Jersey, 2004, pp. 375–378. ISBN 0691114072
19) Shakarian, A.: Application of Monte-Carlo Techniques to the 757/767 Autoland Dispersion Analysis by Simulation, AIAA Paper 83-2193, 1983. https://doi.org/10.2514/6.1983-2193
20) Rubinstein, R. Y. and Kroese, D. P.: *Simulation and the Monte Carlo Method*, 2nd edition, John Wiley & Sons, Inc., New Jersey, 2007, pp. 15–16, 100–101. https://doi.org/10.1002/9780470230381
21) Morelli, E. A. and Klein, V.: *Aircraft System Identification –Theory and Practice–*, 2nd edition, Sunflyte Enterprises, Williamsburg, Virginia, 2016, pp. 115–124. ISBN 9780997430615
22) Mooney, C. Z.: *Monte Carlo Simulation*, Sage Publications Inc., Thousand Oaks, CA, 1997, pp. 46–49. ISBN 0803959435
23) Miyazawa, Y., Nagayasu, M., and Nakayasu, H.: Flight Testing of ALFLEX Guidance, Navigation and Control System, International Council of the Aeronautical Sciences, Paper 98-1.1.3, Sept. 1998.
24) Miyazawa, Y., Motoda, T., Izumi, T., and Hata, T.: Longitudinal Landing Control Law for an Autonomous Reentry Vehicle, *J. Guid. Control Dynam.*, **22**, 6 (1999), pp. 791–800. https://doi.org/10.2514/2.4480
25) Yanagihara, M., Shigemi, M., and Suito, T.: Estimating Aerodynamic Characteristics of Automatic Landing Flight Experiment Vehicle Using Flight Data, *J. Aircraft*, **36**, 6 (1999), pp. 926–933. https://doi.org/10.2514/2.2553
26) Motoda, T.: Robust Optimization of Design Parameters using Monte Carlo Evaluation, JAXA Research and Development Report, RR-22-002, 2022 (in Japanese). http://doi.org/10.20637/00048696

Dongwon Jung
Associate Editor